Accepted Manuscript

Photoresponsive azo-combretastatin A-4 analogues

Shiva K. Rastogi, Zhenze Zhao, Scott L. Barrett, Spencer D. Shelton, Martina Zafferani, Hailee E. Anderson, Madeleine O. Blumenthal, Lindsey R. Jones, Lei Wang, Xiaopeng Li, Craig N. Streu, Liqin Du, William J. Brittain

PII: S0223-5234(17)30905-4

DOI: 10.1016/j.ejmech.2017.11.012

Reference: EJMECH 9887

To appear in: *European Journal of Medicinal Chemistry*

Received Date: 15 August 2017

Revised Date: 25 October 2017

Accepted Date: 4 November 2017

Please cite this article as: S.K. Rastogi, Z. Zhao, S.L. Barrett, S.D. Shelton, M. Zafferani, H.E. Anderson, M.O. Blumenthal, L.R. Jones, L. Wang, X. Li, C.N. Streu, L. Du, W.J. Brittain, Photoresponsive azo-combretastatin A-4 analogues, *European Journal of Medicinal Chemistry* (2017), doi: 10.1016/j.ejmech.2017.11.012.

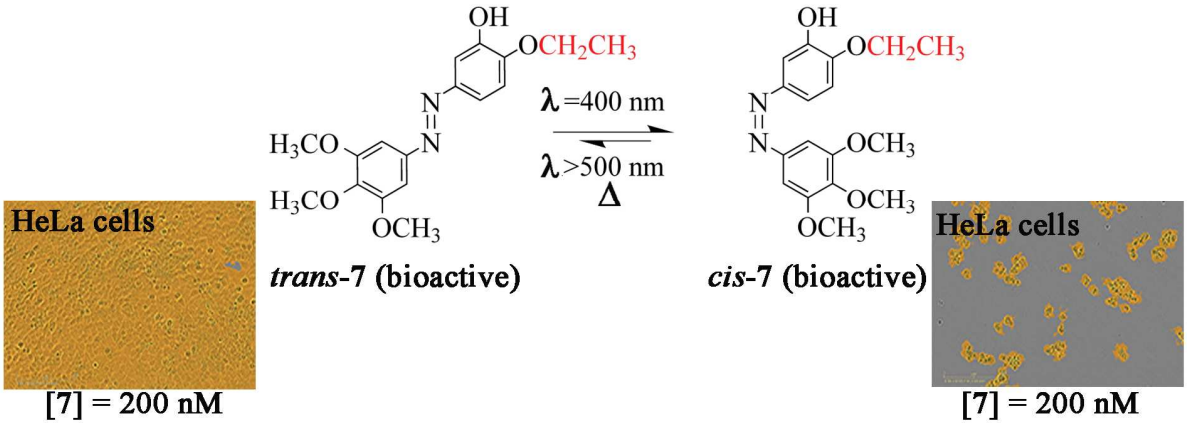

***trans*-7 (bioactive)** ***cis*-7 (bioactive)**

[7] = 200 nM **[7] = 200 nM**

Photoresponsive Azo-Combretastatin A-4 Analogues

Shiva K. Rastogi,[†*] Zhenze Zhao,[†] Scott L. Barrett,[†] Spencer D. Shelton,[†] Martina Zafferani[§], Hailee E. Anderson,[†] Madeleine O. Blumenthal,[†] Lindsey R. Jones,[†] Lei Wang,[‡] Xiaopeng Li,[‡] Craig N. Streu,[§] Liqin Du,[†] and William J. Brittain[†*]

[†]Department of Chemistry and Biochemistry, 601 University Drive, Texas State University San Marcos, TX - 78666, USA, [‡]Chemistry Department, University of South Florida, Tampa, FL – 33620, USA, [§]Department of Chemistry, Albion College, 611 E. Porter Str. Albion, MI - 49224, USA

Abstract

Colchicine analogues in which an azo group is incorporated into a molecule containing the key pharmacophore of colchicine, have found particular utility as switchable tubulin binding chemotherapeutics. Combretastatin is a related compound containing a stilbene fragment that shows different bioactivity for the *cis* and *trans* isomers. We have performed cell assays on 17 new compounds structurally related to a previously reported azo-analogue of combretastatin. One of these compounds showed enhanced potency against HeLa (IC_{50} = 0.11 μM) and H157 cells (IC_{50} = 0.20 μM) for cell studies under 400 nm irradiation and the highest photoactivity (IC_{50} with irradiation/IC_{50} in dark = 550). We have performed docking and physicochemical studies of this new compound (**7**). Kinetic studies in water reveal a longer half-life for the *cis* isomer of **7** which may be one factor responsible for the better IC_{50} values in cell assays and the improved photoresponsive behavior.

Introduction

Photopharmacology is a unique and potentially powerful tool of use for creating more selective cancer-targeting compounds. Biological functions can be controlled by localized application of light that selectively excites photoswitches.[1-3] Light is a non-invasive control element where deleterious toxic effects can be minimized in a qualitative and quantitative manner by adjusting wavelength and intensity respectively.[4-7] One of the chief advantages of light is that it can be supplied with very high spatial and temporal accuracy in biological systems and thus overcome the poor specificity of drug activity.

While this type of dynamic molecular system has great pharmaceutical potential, there are a host of additional considerations inherent to such a system that must be considered when evaluating a potential new therapy. For example, for photopharmaceuticals it is the difference between the biological activity of the excited and unexcited photoswitch that is fundamental to obtaining target selectivity, rather than the absolute potency of the excited photoswitch. In addition, proper evaluation of new photopharmaceuticals requires physicochemical studies to evaluate relative solubilities of active and inactive isomers, or the half-life of the excited state. Both of these properties can impact the observed biological activity and utility of a potential photopharmaceutical.

[Figure 1]
[Figure 2]

One promising area for application of photopharmacology is tubulin polymerization inhibitors.[8] Microtubules are dynamic heterodimeric cytoskeletal structures that are made by self-assembly of α and β-tubulin protein and participate in many cellular functions.[9] The key role of microtubules is in the formation of mitotic spindles during mitotic cell division. Tubulin is the most validated protein target for

small molecules as anti-proliferative and anticancer ligands, which interact with tubulin and disturb microtubule dynamics.[10] In anticancer drug discovery, these ligands are classified into two major categories, first are those that inhibit the polymerization of the mitotic spindle such as vinca alkaloids[11] and colchicine [12,13] (**1**, **Figure 1**) and second are those that inhibit the depolymerization of the mitotic spindle once it has formed, such as paclitaxel.[14] Combretastatin A-4 (CA-4), a stilbene natural product isolated from the stem wood of the South African tree *Combretum caffrum* (**2, Figure 1**),[15] has been investigated extensively for its tubulin polymerization inhibitor activity and was found to possess potent anticancer activity against a number of human cancer cell lines including multidrug resistance cancer cell lines.[16] The X-ray structure of a tubulin complex bound by CA-4 shows that this molecule binds to the colchicine site in tubulin.[17] One disadvantage of CA-4 is its low solubility (0.35 mM),[18] which has prompted the synthesis of the water-soluble phosphate prodrug, combretastatin A-4-phosphate (**3** fosbretabulin disodium, **Figure 1**)[19,20] and amino acid prodrug (**4** ombrabulin, **Figure 1**).[21] Both **3** and **4** are in clinical trials.

CA-4 (**2**) and its prodrugs (**3** and **4**) have been found to be effective anti-angiogenesis agents that inhibit new vascular system development within solid tumors.[22,23] The anti-angiogenic activity of **2** has been widely reported and this activity has been demonstrated to arise from binding to the same site in *β*-tubulin as colchicine.[22,24] However, stilbene compounds are well-known to photoisomerize, and while the *trans* isomer is more stable, the *cis* isomer of CA-4 is orders of magnitude more potent for anticancer activity.[16,25,26] This isomerization limits the stability and shelf-life of CA-4, so much effort has been dedicated to developing conformationally restricted analogues of **2**, in which the *cis*-double bond of **2** is substituted with a heterocyclic ring to prevent isomerization. Some examples of these compounds are azetidinone,[27] *β*-lactum,[28] heteroarylcumarin,[29] benzoxepine,[30] aroylindole,[31] furazane,[32] imidazole,[33] pyrazole,[34] and 1,3-dioxolane.[35] Although these non-isomerizable molecules show better activity against cancer cells growth, drug specificity problems persist because these ligands are also toxic to both normal and healthy cells.

To address issues of tissue selectivity, a photopharmacological azologue of CA-4 in which the stilbene unit of CA-4 is replaced by azobenzene has been reported by Borowjak *et al.*[36] (photostatins), Engdahl *et al.*[37] (azo-combretastatin A4), and later by Sheldon *et al.*[38] (**Figure 2**). Both groups utilized a photopharmacology approach to control the bioactivity of **5** in spatiotemporal manner by substituting azobenzene for the stilbene fragment in CA-4 (substitution of N=N bond for C=C). Compared to stilbene photochemistry, azobenzene has negligible side-reactions during photoisomerization, has lower isomerization activation energy, and abundant literature exists on structural modifications to tune photochemical response. Cellular media are irradiated with ultraviolet light (UV, 395-400 nm) to convert the inactive *trans* isomer of **5** into the bioactive *cis*-**5**.

These promising results prompted our group to investigate these systems, and their physiochemical properties in more detail. Many structure-activity studies on CA-4 have been reported.[31,32] We note that there are recent reports on pharmacophore features for the colchicine binding site[39] and properties of isocombretaquinolines as tubulin inhibitors.[40] It has been demonstrated that the 3,4,5-trimethoxy substituted A-ring of colchicine is required for bioactivity.[26] The principle focus of this study is therefore substituent changes to the B-ring. A key functional group in the B-ring is either a hydrogen bond donating alcohol or amine at the 3-position which gives potent bioactivity and good water solubility.[25] We have synthesized and tested a library of 17 derivatives against two cancer cell lines (HeLa-cervical cancer and H157-lung cancer) in the dark and in presence of

UV light. For the subset with the most promising inhibitory activity, we used a combination of physicochemical analysis and ligand docking simulations to investigate inhibitory differences.

Results and Discussion

Synthesis

We synthesized 17 compounds (**6-22**) for biological testing (see Table 1 and **Figure 3** for structures). Of these, only compounds **21** and **22** have structural changes to the A-ring. These compounds were synthesized by a combination of three principle reactions: 1) azo-coupling of the diazonium salt from either 3,4,5-triemthoxyaniline or 3,4-dimethoxyanline, 2) alkylation of phenol groups, and 3) Pd-catalyzed deprotection of allyl ether protecting group. Details of all synthetic procedures and full characterization (^{1}H NMR, ^{13}C NMR, IR, mp, ESI-HRMS) of all new compounds are available in the supplementary material.

[Figure 3.]

Photochemistry

The photoresponsiveness of all new compounds was studied by UV-visible spectroscopy prior to cellular assay. The photoisomerization of azobenzene compounds is easily monitored by changes in the n-π^* and π-π^* transitions. UV irradiation converted the *trans* isomer to a photostationary state (PSS) within 3-7 min for all compounds. Representative UV-vis spectra are shown in **Figures 4** and **S1**. All compounds showed spectral changes consistent with *trans*-to-*cis* isomerization as evidenced by distinct spectra for the two isomers. Compounds **6**, **16**, **20** and **21** do not display spectral changes upon irradiation because they fall into a class of azobenzenes known as "psedostilbenes."[41] These four compounds all possess a *para*-phenol substituent that participates in a tautomeric equilibrium characterized by extremely fast thermal relaxation of the photoinduced *cis* isomer.[42]

[Figure 4]

Cancer Cell Viability Assays

Seventeen azo-analogues of Azo-CA-4 (**5**) were tested for their antiproliferative activities on HeLa cells as a model for human cervical adenocarcinoma and H157 cells as a model for lung cancer. Series dilutions (from 125 μM to 0.1 nM) of individual azo-compounds were incubated with HeLa and H157 cells for four days in a 96-well plate. The incubated cells in one plate were grown in the dark and in another plate grown in the presence of UV light (390-400 nm, 10 sec irradiation every 34 min). An automated UV light switch system uploaded with html codes on an Arduino board (**Figure S2**) was used for the experiment. The UV light switch setup (Arduino board, 51 LED flash light, bread board, electrical components and power source) was developed as earlier reported.[36]

The activity of azo-compounds on cancer cells was measured via a colorimetric MTT assay (**Figure 5**). The intensity of color correlates to the viability of remaining HeLa and H157 cells; the relative cell viability versus concentration of test compounds were plotted and IC_{50} values determined by curve fitting and statistical analysis (**Figure 6**). Many results have relatively large standard deviations of the mean value. For every MTT assay a new batch of cells (HeLa or H157) was grown and treated with the compounds at the same culture conditions, including cell culture medium, temperature and treatment time. Therefore, the replicates of our MTT assays represent the true biological replicates. Given the

intrinsic heterogeneity of cell populations widely known in cancer cell lines, the large variations in response to compound treatment in different and independent batches of cells are expected, even though the culture condition was strictly controlled. This is an explanation for large standard deviations. The observed variations, however, is of particular importance since it can be used as an estimation of the possible minimum and maximum responses of the cancer line to the compounds that may occur in real biological environments. After analysis of the IC_{50} values of 17 compounds (see **Table 1**) we observed a good structure-activity-relationship (SAR) for compounds **5**, **7** and **8**. Only compounds that displayed activity are included in Table 1. **Figure 3** displays the structure of tested compounds that displayed no detectable activity. Compound **7** with the ethoxy group is the most active ligand in the series and shows 600-fold and 550-fold greater activity in the presence of UV light for HeLa and H157 cells respectively. This is an improvement upon the previously reported azo-CA-4 (**5**) that displays 250-fold and 5-fold enhanced activity following UV light irradiation. Borowjak *et al.*[36] reported 74-fold enhanced activity for **5** for HeLa cell assays, which is comparable to our result. These assay results are supported by white light microscopy of compounds **5**, **7** and **8** (**Figure 7**). Similar results were observed for HeLa and H157 cells where a lower cell count is observed at 200 and 40 nM for compounds **5** and **7** under UV irradiation.

[Table 1]
[Figure 5]
[Figure 6]
[Figure 7]

Physicochemical and Docking Studies

We performed docking and physicochemical studies to investigate the origin of increased potency and increased photochemical effect; i.e., increased ratio of IC_{50}(dark)/ IC_{50}(light). We hypothesized that several factors may be playing a role in explaining the difference between **5** and **7**: 1) stronger binding to the tubulin active site, 2) differential solubility of *cis* and *trans* isomers and/or 3) different half-lives of *cis* isomer.

To address the question of tubulin binding, we performed ligand binding simulations using AutoDock Vina (version 4.2).[43] The tubulin-combretastatin complex (PBD accession number: 5LYJ([17] were converted to required PDBQT files using MGL Tools (version 1.5.6).[44] The default search box size was calculated using the protocol outlined by the authors of Vina. The radius of gyration for ligands *cis*-**5, 7** and **8** was calculated from optimized structures from density functional theory (B3LYP/6-311+G(d) as implemented in Gaussian 09[45]) and used to estimate box size. **Figure 8** shows an overlay of **2** in the bound state and the lowest energy binding conformations of **5** and **7**. Azo compounds **5** and **7** have nearly identical binding conformations and closely overlap the X-ray binding structure of combretastatin. The RMSD for comparison of docking pose of combretastatin versus the X-ray structure was 0.14 nm. The distance between the stilbene double bond and the azo group is 0.1 nm for best docking poses of **2** versus **5** and **7**. One difference between combrestastatin A4 and azo compound **5** and **7** is the orientation of the *para*-methoxy group on the A-ring. The calculated binding affinity obtained via Vina was -8.1, -7.6, and -7.1 kcal/mol for **5, 7** and **8** for the lowest energy conformer. Visualization of the binding conformations and binding energies do not indicate a significant difference in the binding affinity of **5** versus **7.**

[Figure 8]

The aqueous solubility of azobenzene compounds is generally sub-mM and the *cis* isomer can be 50-times more soluble than *trans*.[46] Aqueous solubility will decrease with an increasing number of carbon atoms so it is expected that S_w (water solubility) will decrease in the order **5** > **7** > **8**. However, we could not predict *cis*/*trans* differential solubility nor the half-lives of the *cis* isomers of **5**, **7** and **8**. **Table 2** contains kinetic data on the thermal *cis*-to-*trans* isomerization and S_w values for *cis* and *trans* isomers. Both of these physicochemical characteristics could potentially affect the effective concentration of the bioactive *cis* isomer. The values for S_w (*cis*) correspond to photostationary states (PSS) and thus represent lower limits for S_w. To put the data for **5**, **7** and **8** into perspective, several literature examples are included in the **Table 2**. From the data in **Table 2**, we observed the expected order of aqueous solubility where **5** possesses the highest S_w for both isomers. The modest difference in *cis*/*trans* solubility for **5**, **7** and **8** is not general for less substituted azobenzenes and can be understood by comparison of calculated dipole moments. We calculated dipole moments (**Table S2,** supplementary material) using density functional theory and have observed that there is a correlation between $\Delta\mu$ and ΔS_w as exemplified by 4-trifluoroazobenzene where $\Delta\mu$ is negative and this is reflected in equivalent solubility for the geometric isomers. The activity of these compounds is related to concentration of active species and binding affinity to tubulin. Sparingly soluble compounds in water potentially have stronger hydrophobic interactions with the protein so it can be argued the lower solubility of **7** relative to **5** may be associated with stronger binding to active site.

We studied the half-life for the *cis* isomer of compounds **5** and **7** via 500 MHz ^{1}H NMR. We attempted to use UV-Vis spectroscopy to measure the kinetics of the thermal *cis*-to-*trans* isomerization. However, we obtained inconsistent results due to precipitation of these sparingly soluble compounds. We have previously studied *cis*/*trans* ratios of azobenzene compounds in water,[46] and the low solubility of such derivatives requires long acquisition times making these experiments difficult and prone to trace impurities. Kinetics studies in methanol-d_4 revealed nearly identical isomerization rates for **5, 7** and **8**. Kinetics studies in water were replicated and limited to **5** and **7.** The first-order rate plots are provided in the supplementary material (**Tables S5** and **S6)**. Surprisingly, the rate of isomerization for **5** is 3-fold greater than **7** when measured in water, which corresponds to half-lives of 138 and 46 h, respectively for **5** and **7**. This rate difference is unexpected given the minor and remote structural difference between **5** and **7**. Density functional theory (**Table S3**) and rate measurements in methanol-d_4 support equivalent reactivity for all three compounds. The half-lives for **5** and **7** may be a reflection of differential solubility for the *cis* and *trans* isomers. This effect has been reported recently and is pronounced for the parent azobenzene compound where $S_w(cis)/S_w(trans) = 40$ leading to longer-lived *cis* populations. Regardless of the origin of the experimentally observed rate difference, the resulting difference in half-lives is one potential factor that explains the different potency and photoresponsive behavior of compounds **5** and **7.**

Conclusion

In summary, we have synthesized a library of photoswitchable anologues of the known tubulin-binding photoswitch **5**, measured their photoisomerization, and evaluated their light induced cytotoxicity in two human cancer cell lines. These studies yielded a novel compound (**7**) that demonstrates a greater biological activity and relative improvement in activity upon irradiation than the previously reported compound (**5**) in both HeLa and H157 cells. Molecular modeling suggests that this compound binds within the colchicine binding pocket of tubulin. To characterize the physiochemical behavior of **7**, and in an attempt to explain its improved bioactivity upon irradiation, the thermal *cis*-to-t*rans* half-life, as well

as the dipole moments and water solubility of the *cis* and *trans* isomers were measured. The reduced water solubility of *cis*-7 with respect to *cis*-**5** may explain its improved potency, as desolvation upon binding tubulin would be predicted to be energetically favored for the less water soluble compound. Additionally, an experimentally observed longer half-life for *cis*-**7** relative to *cis*-**5** has been identified as one potential factor for the observed difference in activity.

Acknowledgment

Albion College Faculty Development Fund and the Foundation for Undergraduate Research, Scholarship, and Creative Activity (FURSCA) for funding. We thank the National Science Foundation (PREM Center for Interfaces, DMR-1205670) for financial support of this research. The authors also acknowledge the support of the National Science Foundation for NMR instrumentation (CR1IF:MU-0946998 and MRI-0821254).

References

[1] Fehrentz, T.; Schonberger, M.; Trauner, D. Optochemical Genetics *Angew. Chem. Int. Ed.* **2011**, *50*, 12156-12182.
[2] Velema, W. A.; Szymanski,W.; Feringa, B. L. Photopharmacology: Beyond Proof of Principle *J. Am. Chem. Soc.* **2104**, *135*, 2178-2191.
[3] Broichhagen, J.; Frank, J. A.; Trauner, D. A Roadmap to Success in Photopharmacology, *Acc. Chem. Res.* **2015**, *48*(7), 1947-1960.
[4] Syzmanski, W.; Beierle, J. M.; Kistemaker, H. A. V.; Velma W. A.; Feringa, B. L. Reversible Photocontrol of Biological Systems by the Incorporation of Molecular Photoswitches, *Chem. Rev.* **2013**, *113*, 6114-6178.
[5] Brieke, C.; Rohrbach, F.; Gottschalk, A.; Mayer, G.; Heckel, A. Light-Controlled Tools *Angew. Chem. Int. Ed.* **2012**, *51*, 8446-8476.
[6] Beharry, A. A.; Woolley, G. A. Azobenzene Photoswitches for Biomolecules *Chem. Soc. Rev.* **2011**, *40*, 4422-4437.
[7] Mayer, G.; Heckel, A. Biologically Active Molecules with a "Light Switch", *Angew. Chem. Int. Ed.* **2006**, *45*, 4900-4921.
[8] Borowiak, M.; Nahaboo, W.; Reynders, M.; Nekolla, K.; Jalinot, P; Hasserodt, J.; Rehburg, M.; Delatree, M.; Zahler, S.; Vollamar, A.; Trauner, D. Photoswitchable Inhibitors of Microtubule Dynamics Optically Control Mitosis and Cell Death *Cell* **2015**, *162*(2), 403-411.
[9] Downing, K. H.; Nogales, E. Tubulin and Microtubulin Structure. *Curr. Opin. Cell Biol.* **1998**, *10*(1), 16-22.
[10] Jordan, M. A. Mechanism of Action of Antitumor Drugs that Interact with Microtubules and Tubulin *Current Medicinal Chemistry-Anti-Cancer Agents* 2, **2002**, *2*(1), 1-17.
[11] Hardfield, J. A.; Ducki, S.; Hirst, N.; McGown, A. T. Tubulin and Microtubules Agents for Anticancer Drugs *Progress in Cell Cycle Research* **2003**, *5*, 309-325.
[12] Bhattacharyya, B.; Panda, D.; Gupta, S.; Banerjee, M. Anti-Mitotic Activity of Colchicine and the Structural Basis for its Interaction with Tubulin *Med. Res. Rev.* **2008**, *28*(1), 155-183.
[13] Margolis, R. L.; Rauch, C. T.; Wilson, L. Mechanism of Colchicine-Dimer Addition to Microtubule Ends: Implication for the Microtubules Polymerization Mechanism *Biochem.* **1980**, *19*, 5550-5557.
[14] Dumontet, C.; Jordan, M. A. Microtubule-Binding Agents: A Dynamic Field of Cancer Therapeutics *Nat. Rev. Drug Discov.* **2010**, *9*, 790.
[15] Watt, J. M.; Gerdina, M. The Medicinal and Poisonous Plants of Southern and Eastern Africa, E. & S. Livingston Ltd.: Edenburg and London, U.K., 1962.
[16] Pettit, G. R.; Rhodes, M. R.; Herald, D. L.; Hamel, E.; Schemidt, J. M.; Pettit, R. K. Antineoplastic Agent. 445. Synthesis and Evaluation of Structural Modification of of (*Z*)- and (*E*)-Combretastatin A-41, *J. Med. Chem.* **2005**, *48*, 4087-4099.

[17] Gaspari, R.; Prota, A. E.; Bargsten, K.; Cavalli, A.; Steinmetz, M.O. Structural Basis of cis-and trans-Combretastatin Binding to Tubulin *Chem.* **2017**, *2*(1), 102-113.
[18] Lee, M.; Brockway, O.; Dandavati, A.; Tzou, S.; Sjoholm, R.; Nickols, A.; Babu, B.; Chavda, S.; Satam, V.; Hartley, R. M.; Westbrook, C. Design and Synthesis of Novel Enhanced Water Soluble Hydroxyethyl Analogs of Combretastatin A-4. *Bioorg. Med. Chem. Lett.* **2011**, *21*(7), 2087-2091.
[19] Cooney, M. M.; Ortiz, J.; Bukowski, R. M.; Remick, S. C. Novel Vascular Targeting/Disrupting Agents: Combretastatin A4 Phospate and Related Compounds. *Curr. Oncol. Rep.* **2005**, *7*(2), 90-95.
[20] https://clinicaltrials.gov/ct2/show/NCT00060242?term=NCT00060242&rank=1.
[21] Ohsumi, K.; Hatanaka, T.; Nakagawa, R.; Fukuda, Y.; Morinaga, Y.; Suga, Y.; Nihei, Y.; Ohishi, K.; Akiyama, Y.; Tsuji, T.; Synthesis and Antitumor Activities of Amino Acid Prodrugs of Amino-Combretastatins. *Anti-Cancer Drug Design* **1999**, *14*, 539-548.
[22] Dark, G. G.; Hill, S. A.; Prise, V. E.; Tozer, G. M.; Pettit, G. R.; Chaplin, D. J.; Combretastatine A-4 and Agent That Displays Potent and Selective Toxicity Towards Tumor Vasculature *Cancer Res.*, **1997**, *57* (10), 1829-1834.
[23] Sessa, C.; Lorusso, P.; Tolcher, A.; Farace, F.; Lassau, N.; Delmonte, A.; Braghetti, A.; Bahleda, R.; Cohen, P.; Hospitel, M.; Veyrat-Follet, C.; Soria, J. C. Phase I Safety, Pharmacokinetic and Pharmacodynamic Evaluation of the Vascular Disrupting Agent Ombrabulin (AVE8062) in Patients With Advanced Solid Tumors *Clin. Cancer Res.*, **2013**, *19*, 4832-4842.
[24] Prota A. E.; Danel, E.; Bachmann, F.; Bargstem, K.; Buey, R. M.; Pohlmann, J.; Reinelt, S.; Lane, H.; Steimetz, M. O. The Novel Microtubule-Destabilizing Drug BAL27862 Bind to the Colchicine Site of Tubulin with Distinct Effects on Microtubule Organization. *J. Mol. Biol.* **2014**, *426*, 1848-1860.
[25] Ohsumi, K.; Hatanaka, T.; Fujita, K.; Nakagawa,R.; Fukuda,Y.; Nihei, Y.; Suga, Y.; Morinaga, Y.; Akiyama, Y.; Tsuji, T. Syntheses and Antitumor Activity of *Cis*-Restricted Combretastatins: 5-Membered Heterocyclic Analogues. *Bioorg. Med. Chem. Lett.* **1998**, *8* (22), 3153-3158.
[26] Cushman, M.; He, H. M.; Lin, C. M.; Hamel, E. Synthesis and Evaluation of a Series of Benzylaniline Hydrochlorides as Potential Cytotoxic and Antimitotic Agents Acting by Inhibition of Tubulin Polymerization. *J. Med. Chem.* **1993**, *36* (19), 2817-2821.
[27] O'Boyle, N. M.; Carr, M.; Greene, L. M.; Bergin, O.; Nathwani, S. M.; McCabe, T.; Lloyd, D. G.; Zisterer, D. M. and Meegan, M. J. Synthesis and Evaluation of Azetidinone Analogues of Combretastatin A-4 as Tubulin Targeting Agents, *J. Med. Chem.* **2010**, 53, 8569–8584.
[28] Banik, I.; Becker, F. F.; Banik, B. K. Stereoselective Synthesis of Beta-Lactams with Polyaromatic Imines: Entry to New and Novel Anticancer Agents. *J. Med. Chem.* **2003**, *46* (1), 12-15.
[29] Ganina, O. G.; Daras, E.; Bourgarel-Rey, V.; Peyrot, V.; Andresyuk, A. N.; Finet, J. P.; Fedorov, A. Y.; Beletskaya, I. P.; Combes, S. Synthesis and Biological Evaluation of Polymethoxylated 4-Heteroarylcoumarins as Tubulin Assembly Inhibitor. *Bioorg. Med. Chem.* **2008**, *16* (19), 8806-8812.
[30] Barrett, I.; Carr, M.; O'Boyle, N.; Greene, L. M.; Knox, A., J. S.; Lloyd, D. G.; Zisterer, D. M.; Meegan, M. J. Lead Identification of Conformationally Restricted Benzoxepin Type Combretastatin Analogs: Synthesis, Antiproliferative Activity, and Tubulin Effects *J. Enzym. Inhib. Med. Ch.* **2010**, *25* (2), 180-194.
[31] Liou, J. P.; Chang, Y. L.; Kuo, F. M.; Chang, C. W.; Tseng, H. Y.; Wang, C. C.; Yang, Y. N.; Chang, J. Y.; Lee, S. J.; Hsieh, H. P. Concise Synthesis and Structure-Activity Relationships of Combretastatin A-4 Analogues,1-Aroylindoles and 3-Aroylindoles, as Novel Classes of Potent Antitubulin Agents. *J. Med. Chem.* **2004**, *47* (17), 4247-4257.
[32] Tron, G. C.; Pirali, T.; Sorba,G.; Pagliai, F.; Busacca,S.; Genazzani, A. A. Medicinal Chemistry of Combretastatin A4: Present and Future Directions. *J. Med. Chem.* **2006**, *49* (11), 3033-3044.
[33] Wang, L.; Woods, K. W.; Li, Q.; Barr, K. J.; McCroskey, R. W.; Hannick, S. M.; Gherke, L.; Credo, R. B.; Hui, Y. H.; Marsh, K.; Warner, R.; Lee, J. Y.; Zielinski-Mozng, N.; Frost, D.; Rosenberg, S. H.; Sham, H. L. Potent, Orally Active Heterocycle-Based Combretastatin A-4

Analogues: Synthesis, Structure-Activity Relationship, Pharmacokinetics, and In Vivo Antitumor Activity Evaluation. *J. Med. Chem.* **2002**, *45*, 1697-1711.

[34] Ohsumi, K.; Hatanaka, T.; Fujita, K.; Nakagawa, R.; Fukuda,Y.; Nihei, Y.; Suga, Y.; Morinaga, Y.; Akiyama, Y.; Tsuji, T. Syntheses and Antitumor Activity of Cis-Restricted Combretastatins: 5-Membered Heterocyclic Analogues. *Bioorg. Med. Chem. Lett.* **1998**, *8* (22), 3153-3158.

[35] Shirai, R.; Takayama, H.; Nishikawa, A.; Koiso, Y.; Hashimoto, Y. Asymmetric Synthesis of Antimitotic Combretadioxolane with Potent Antitumor Activity Against Multi-Drug Resistant Cells *Bioorg. Med. Chem. Lett.* **1998**, *8* (15), 1997-2000.

[36] Borowiak, M.; Nahaboo, W.; Reynders, M.; Nekolla, K.; Jalinot, P.; Hasserodt, J.; Rehberg, M.; Delattre, M.; Zahler, S.; Vollmar, A.; Trauner, D.; Thorn-Seshold, O. Photoswitchable Inhibitors of Microtubule Dynamics Optically Control Mitosis and Cell Death. *Cell* **2015**,*162* (2), 403-411.

[37] Engdahl, A. J.; Torres, E. A.; Lock, S. E.; Engdahl, T. B.; Mertz, P. S.; Streu, C. N. Synthesis, Characterization, and Bioactivity of the Photoisomerizable Tubulin Polymerization Inhibitor azo-Combretastatin A4, *Org. Lett.* **2015**, *17*, 4546−4549.

[38] Sheldon, J. E.; Dcona, M. M.; Lyons, C. E.; Hackett, J. C.; Hartman, M.C. Photoswitchable Anticancer Activity via Trans–Cis Isomerization of a Combretastatin A-4 Analog *Org. Biomol. Chem.* **2016**, *14*(1), 40-49.

[39] Mangiatordi, G. F.; Trisciuzzi, D.; Alberga, D.; Denora, N.; Iacobazzi, R. M.; Gadaleta, D.; Catto, M.; Nicolotti, O. Novel Chemotypes Trageting Tubulin at the Colchicene Binging Site and Unbiasing P-gycloprotein *Eur. J. Med. Chem.* **2017**, *139*, 792-803.

[40] Khelifi, I.; Naret, T.; Renko, D.; Hamze, A.; Bernadat, G.; Bignon, J.; Lenoir, C.; Dubois, J.; Brion, J.-D.; Revot, O. Design, Synthesis and Anticancer Properties of IsoCombretaQuinolines as Potent Tubulin Assembly Inhibitors *Eur. J. Med. Chem.* **2017**, *127*, 1025-1034.

[41] Dhammika Bandara, H. M.; Burdette, S. C. Photoisomerization in Different Classes of Azobenzene *Chem. Soc. Rev.*, **2012**, *41*, 1809-1825.

[42] Gabor, G.; Fischer, E. Spectra and Cis-Trans Isomerism in Highly Bipolar Derivatives of Azobenzene *J. Phys. Chem.* **1971**, *75*, 581-583.

[43] Trott, O.; Olson, A. J. AutoDock Vina: improving the speed and accuracy of docking with a new scoring function, efficient optimization, and multithreading Trott, O. and Olson, A.J. *J. Comput. Chem.* **2010**, *31*, 455-461.

[44] Morris, G.M.; Huey, R.; Lindstrom, W.; Sanner, M. F.; Belew, R. K.; Goodsell, D. S.; Olson, A. J. AutoDock4 and AutoDockTools4: Automated docking with selective receptor flexibility. *J. Comput. Chem.* **2009**, *30*, 2785-2791.

[45] M. J. Frisch, G. W. Trucks, H. B. Schlegel, G. E. Scuseria, M. A. Robb, J. R. Cheeseman, G. Scalmani, V. Barone, B. Mennucci, G. A. Petersson, H. Nakatsuji, M. Caricato, X. Li, H. P. Hratchian, A. F. Izmaylov, J. Bloino, G. Zheng, J. L. Sonnenberg, M. Hada, M. Ehara, K. Toyota, R. Fukuda, J. Hasegawa, M. Ishida, T. Nakajima, Y. Honda, O. Kitao, H. Nakai, T. Vreven, J. A. Montgomery, Jr., J. E. Peralta, F. Ogliaro, M. Bearpark, J. J. Heyd, E. Brothers, K. N. Kudin, V. N. Staroverov, R. Kobayashi, J. Normand, K. Raghavachari, A. Rendell, J. C. Burant, S. S. Iyengar, J. Tomasi, M. Cossi, N. Rega, N. J. Millam, M. Klene, J. E. Knox, J. B. Cross, V. Bakken, C. Adamo, J. Jaramillo, R. Gomperts, R. E. Stratmann, O. Yazyev, A. J. Austin, R. Cammi, C. Pomelli, J. W. Ochterski, R. L. Martin, K. Morokuma, V. G. Zakrzewski, G. A. Voth, P. Salvador, J. J. Dannenberg, S. Dapprich, A. D. Daniels, O. Farkas, J. B. Foresman, J. V. Ortiz, J. Cioslowski, D. J. Fox, D. J. *Gaussian 09, Revision A.1*; Gaussian, Inc.: Wallingford, CT, 2009.

[46] Brown, C.; Rastogi, S. K.; Barrett, S. L.; Anderson, H. E.; Twichell, E.; Gralinski, S.; McDonald, A.; Brittain, W. J. Differential Azobenzene Solubility Increases Equilibrium Cis/Trans Ratio in Water *J. Photoch. Photobio. A* **2017**, *336*, 140-145.

[47] Nakano, M.; Uematsu, Y.; Arita, T. Solution and Partition Behaviors of Colchicine *Chemical and Pharmaceutical Bulletin* **1977**, *25*(5), 1109-1112.

FIGURE CAPTIONS

Figure 1. Natural product and synthetic tubulin polymerization inhibitors: colchicine (**1**), *cis*- and *trans*-forms of combretastatin A-4 (**2**) and related compounds, CA-4 phosphate (**3**) and amino-acid derivative of CA-4 (**4**).

Figure 2. Tubulin polymerization inhibition profile for azo-combretastatin A-4 (**5**) and analogues **6, 7, 8**.

Figure 3. Structures of compounds that showed no detectable activity in MMT cell assays.

Figure 4. UV-Visible photo-isomerization of compounds **5** (a), **6** (b), **7** (c) and **8** (d) in DMSO at 0.01mg/mL concentration.

Figure 5. MTT assay of HeLa (left) and H157 (right) cells in the presence of 200 nM (a) and 40 nM (b) of compounds **5**, **7** and **8** in dark and in the presence of 400 nm isomerizing light.

Figure 6. Relative cell viability vs. concentration graphs of Azo-CA4 **5** and analogues **6**, **7**, and **8** for two cancer cell lines, HeLa (left column) and H157 cells (right column).

Figure 7. White light microscopy (phase contrast images using confluence mask of gold color) of HeLa cells incubated 72 h with DMSO and compounds **5**, **7** and **8** at concentrations of (a) 200 nM and (b) 40 nM. Images are shown for samples in the dark versus 400 nm irradiation.

Figure 8. AutoDock 4.2 Vina results for the most stable binding conformation of combretastatin A4 (a), **5** (b) and **7** (c)**.**

Table 1. IC_{50} values[a] (μM) and dark vs UV ratio of IC_{50} of Azo-CA4 and analogues that display bioactivity in dark and/or in UV (395 nm) from MTT assay (ND=not detected).

Entry	Structure[b] Ar_B	HeLa Cells			H157 Cells		
		Dark	UV	Dark/UV	Dark	UV	Dark/UV
5	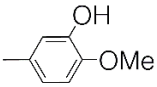	50 ± 20	0.16 ± 0.07	310 ± 20	50 ± 40	0.16 ± 0.03	310 ± 40
6	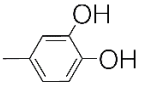	30 ± 30	0.34 ± 0.16	80 ± 30	10 ± 2	1.9 ± 1.4	5 ± 2
7	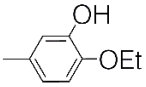	60 ± 30	0.11 ± 0.03	550 ± 30	110 ± 60	0.2 ± 0.1	550 ± 60
8	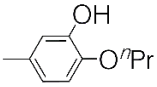	ND	3 ± 2		ND	2 ± 2	
9	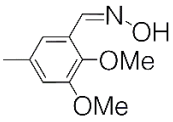	23 ± 16	36 ± 25	~ 1[c]	ND	ND	-
13	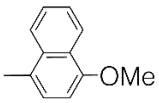	ND	ND	-	90 ± 60	100 ± 70	~ 1[c]
16	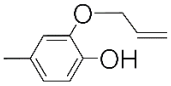	60 ± 20	ND	-	ND	ND	-
17	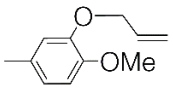	ND	53 ± 14	-	ND	ND	-
20	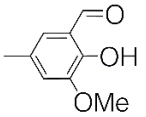	14 ± 7	12 ± 5	~ 1[c]	18 ± 1	5.3 ± 0.3	3 ± 1
21	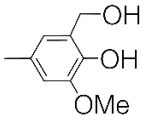	21 ± 15	15 ± 10	~ 1[c]	ND	ND	-
22	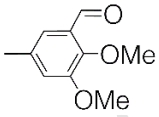	9 ± 7	13 ± 3	~ 1[c]	10 ± 10	3.6 ± 0.3	~ 1[c]
1		Colchicene	0.003 ± 0.001 (dark)		0.010 ± 0.003 (dark)		

[a] Reported numbers are mean values ± standard deviation. b Ar_A-N=N-Ar_B where structure of the A-Ring (Ar_A) = 3,4,5-trimethoxyphenyl. [c] Ratio can only be expressed as an order of magnitude because standard deviation was larger than the mean.

Table 2. Solubility and half-life data for azobenzene compounds in water at 23°C.

Compound	**S_w, mM**		**S_w(*cis*)/ S_w(*trans***	**$\tau_{1/2}$, h**
	Cis	***Trans***		
Azobenzene[a]	2	0.05	40	48
4-methoxyazobenzene	2	0.09	22	6
4-trifluoromethylazobenzene	0.02	0.02	1	nd[d]
Azobenzene-*L*-Leu-*L*-Pro[a]	14	0.3	47	24
5	0.07	0.03	2	46 (7)[e]
7	.04	.02	2	138 (8)[e]
8	.02	.01	2	nd[d] (9)[e]
Colchicine[b]		41.6		
Combretastatin **2**[c]		0.35		

[a] Reference 46. [b] Reference 47. [c] Reference 18. [d] Not determined. [e] Half-life in methanol.

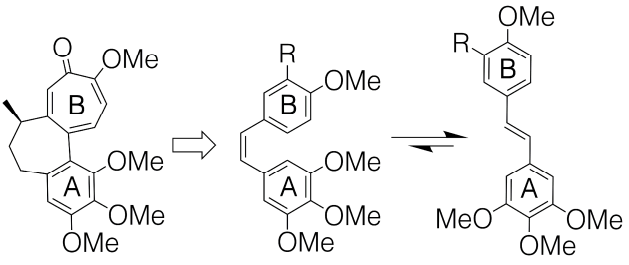

Colchicine **1** *cis* (bioactive) *trans* (inactive)

2: R=OH; Combretastatin A-4 (CA-4)
3: R=OPO_3Na_2; Fosbretabulin (CA-4P)
4: R=NH-CO-CH(NH_2)(CH_2OH); Ombrabulin

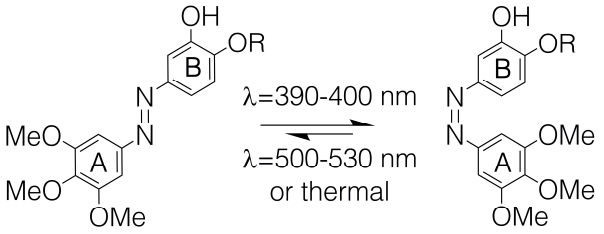

trans (inactive)

5: R=Me
6: R=H
7: R=Et
8: R=*n*-Pr

cis (bioactive)

trans→*cis* bioactivity increase

5: *cis* 310x more active
6: *cis* 5-80x more active
7: *cis* 550x more active
8: no dark activity detected

A-Ring B-Ring

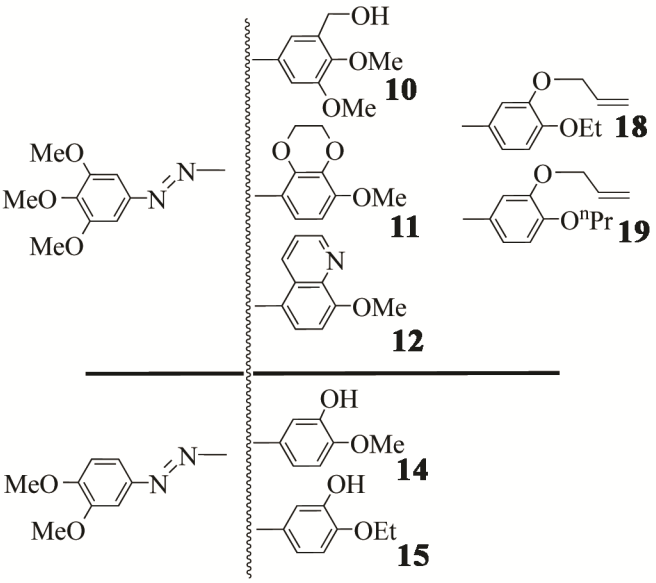

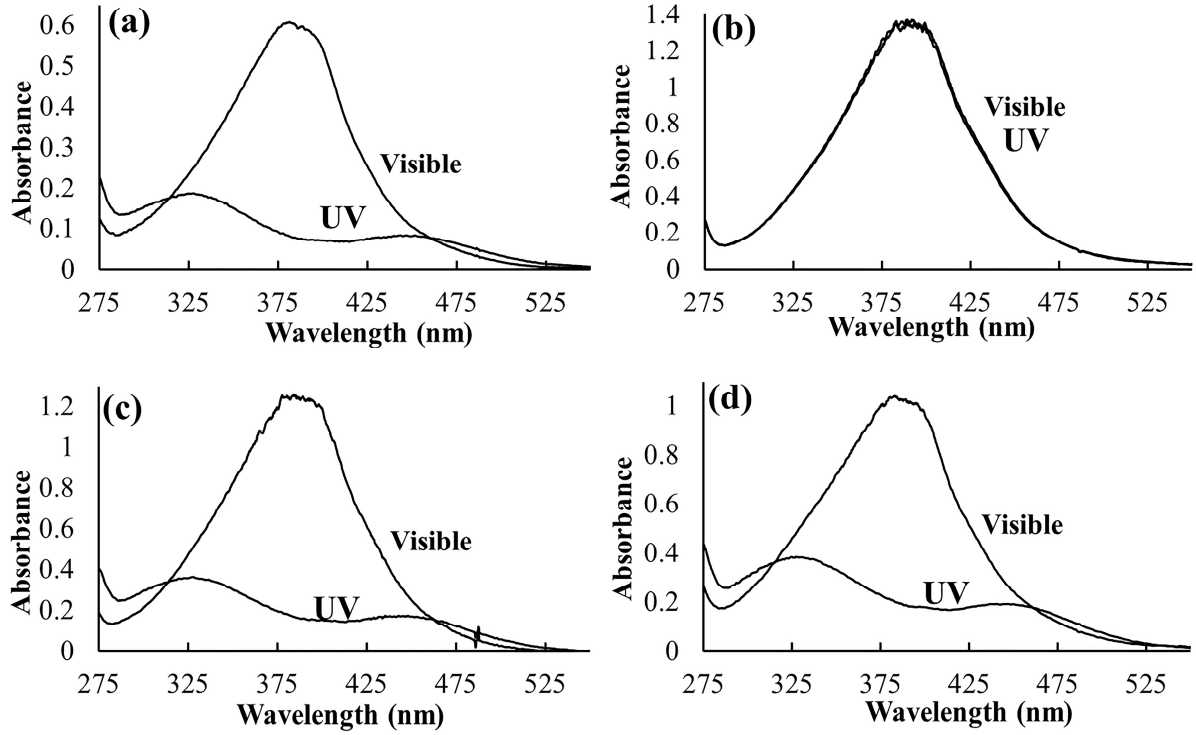

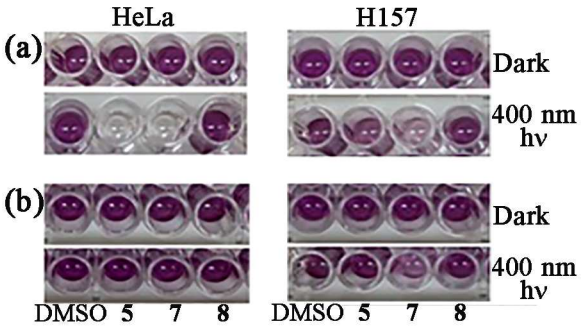

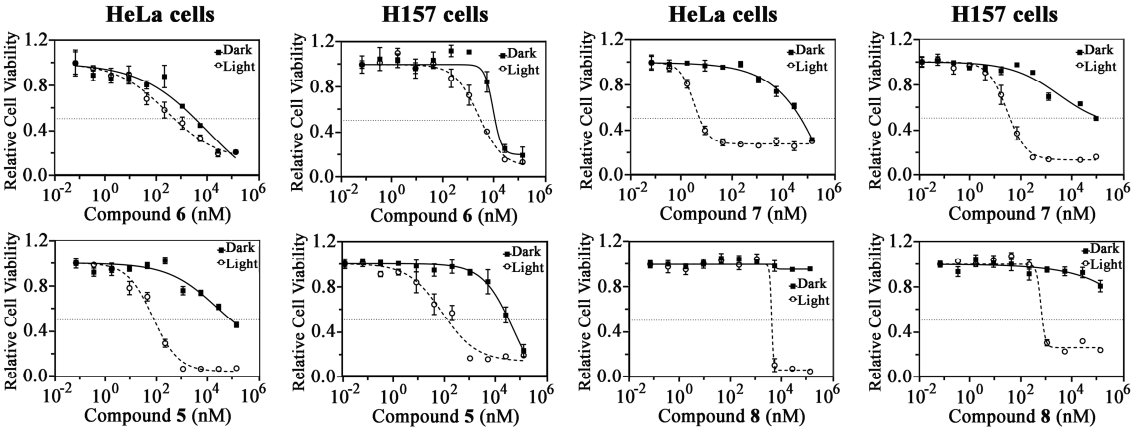

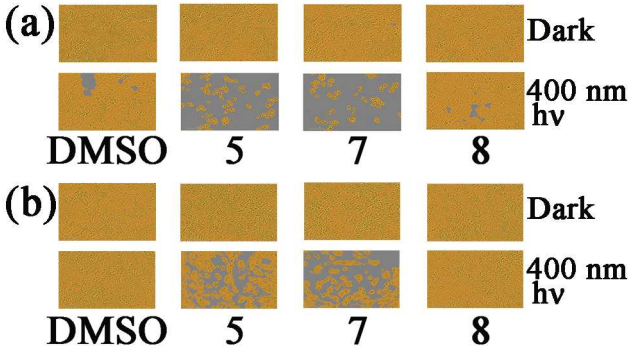

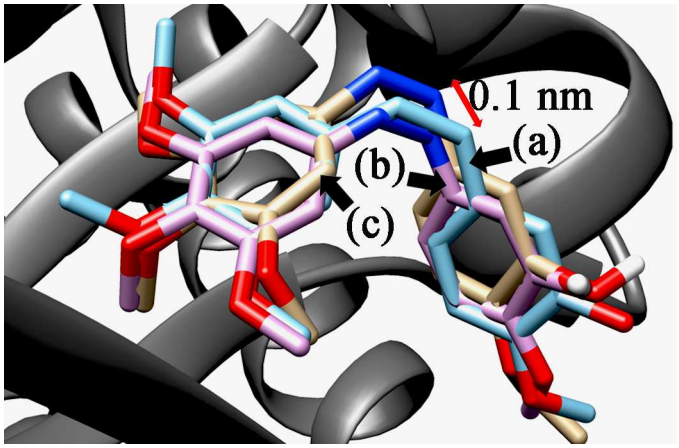

Highlights

- Seventeen analogs of azocombretastatin A-4 were tested for photopharmacological activity against HeLa and H157 cell lines
- Compound **7** displayed ~2x improved activity relative to previously reported A-4 (compound **5**)
- The structural difference between **7** and **5** is an ethoxy substitution for methoxy on the A-ring
- The hypothesis to account for this improved activity is based on differential aqueous solubility of *cis* and *trans* isomers